

DOI: <http://doi.org/10.21698/simi.2018.fp07>

NANOSCALE IRON PARTICLES FOR WASTEWATER DECONTAMINATION

Eugenia Panturu¹, Razvan Ioan Panturu², Gheorghita Jinescu³, Antoneta Filcenco – Olteanu¹,
Aura Daniela Radu¹

¹National Research & Development Institute for Metals and Radioactive Resources-ICPMRR,
70 Carol I Blvd., 0209917, Bucharest, ioanpanturu@yahoo.com, Romania

²Honeywell, 169A Calea Floreasca, 014459, Bucharest, Romania

³University Politehnica of Bucharest, Chemical and Biochemical Engineering Department,
Polizu Street no.1-6, Bucharest, Romania

Abstract

This paper described the equilibrium and the kinetic of uranium adsorption from waste water using activated carbon without/with nano-iron impregnated, applying batch method. Adsorption isotherms of uranium equilibrium are analysed with Freundlich isotherms which reveal high affinity to activated carbon impregnated with nano-iron compared to nonimpregnate. Kinetic study showed that the decisive step of the uranium adsorption process rate is the intraparticle diffusion.

Keywords: *activated carbon, adsorption isotherms, diffusion, nano-iron, uranium*

Introduction

A wide range of methods are available for removal of heavy metal ions from aqueous solutions. These include ion exchange, solvent extraction, reverse osmosis, precipitation, filtration, electrochemical treatment, adsorption etc. The most studied and applied method was the adsorption process. A number of researchers have used a variety of adsorbents to remove heavy metal ions from aqueous solutions such as activated carbon, bentonites, zeolites, iron oxides, clays etc. (Akperov & Maharramov 2010, Alic & Manea 2013, Bratkova & Angelov 2013, Erust & Sahin 2014, Mas Haris & Abdul Wahab 2011, Oprčkal & Mladenović 2017, Hu & Wang 2011). Research on the radioactive pollutants removal from the wastewater by adsorption processes using nano-iron or nano-iron impregnated solid support, gain a more general interest. In the early 1990s, the reducing capabilities of metallic substances, such as zero-valent iron, began to be examined for their ability to treat a wide range of contaminants in hazardous waste water. The small particle size and high surface area to mass ratio make iron nanoparticles highly reactive and extremely versatile. The high surface area and surface reactivity compared with granular forms enable the nanoparticles to remediate more material at a higher rate and with a lower generation of hazardous by-products (Zhang 2003). The ability of the nanoparticles to act as strong reducers also enables the remediation of an extremely wide range of contaminants. It proved to be particularly suitable for the decontamination of halogenated organic compounds, but subsequent studies have confirmed the possibility of using zero-valent iron in aim to the reduction of: nitrate, bromated, chlorate, nitro aromatics compounds, brominated pesticides. Zero-valent iron proved to be effective in removing arsenic, lead, uranium and hexavalent chromium (Alvarado & Rose 2010, Dickinson & Scott 2010, Gheju 2011,

MacFarlane & Payton 2014, Mamadou & Duncan 2013, Eglal & Ramamurthy 2015, Panturu et al 2010, and Panturu et al 2011). In 1997 Wang and Zhang (Wang & Zhang 1997) first produced the nanoscale iron particles in the laboratory using the method of sodium borohydride reduction. This work aimed to study equilibrium and kinetics of adsorption of uranium from wastewater, using as adsorbent material simple activated carbon Purolite AG 20 G and impregnated with nano-iron.

Materials and Methods

Synthesis of activated carbon Purolite type AG 20 G (from Purolite Company, Romania) impregnated with nano-iron was done by the method of reduction of iron ions (III) by sodium borohydride in the presence of sodium hydroxide, resulting in a coal with a nano-iron content of 5.99%. To study the equilibrium of the U (VI) ions adsorption process, well-defined quantity of activated carbon Purolite type 20G AG without/with impregnated nano-iron was put in contact with solutions, in the glass bottles containing uranium with varying initial concentration, C (g U L^{-1}), a solid: liquid ratio of 1:10 (wt.). The solutions pH, determined with a pH meter InoLab was adjusted to 8 ± 0.2 values. Samples were kept under stirring at constant temperature 25 ± 1 °C in a thermostat type bath shaker to achieve balance. The two phases were separated by filtration. Scanning Electron Microscopy method was made with an electronic microscope Quanta Inspect F and particle size analysis was performed with Zetasizer Nano ZS ZEN device 3600. The analyses have highlighted the absence and presence of iron nano-particles (average size of 211.5 nm) on the activated carbon (Figure 1-2).

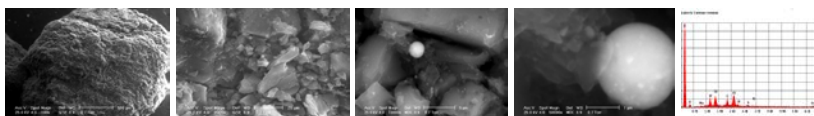


Figure 1. Activated carbon – initial structure and composition

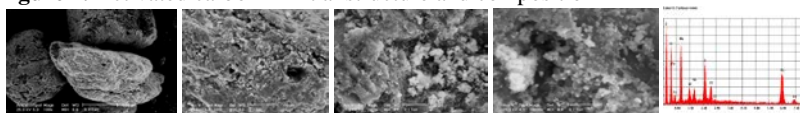


Figure 2. Nano-iron on activated carbon, structure and composition

Results and Discussion

Adsorption Isotherms

Freundlich isotherm (Khan 2012), which describes processes detention of U (VI) ions on adsorbent materials, used for this study, is described by the Equation (1):

$$q_e = K_f \cdot C_e^{1/n} \quad (1)$$

where q_e (g U kg^{-1}) is the amount of adsorbed material retained on adsorbent unit, C_e (gUL^{-1}) is the equilibrium concentration of the contaminant in aqueous solution and K_f and n are Freundlich constants which correspond to adsorption capacity.

For interpretation of the balance (Figure 3) was used Freundlich isotherm in the linear form Equation (2):

$$\log q_e = \log K_f + \left(\frac{1}{n}\right) \log C_e \quad (2)$$

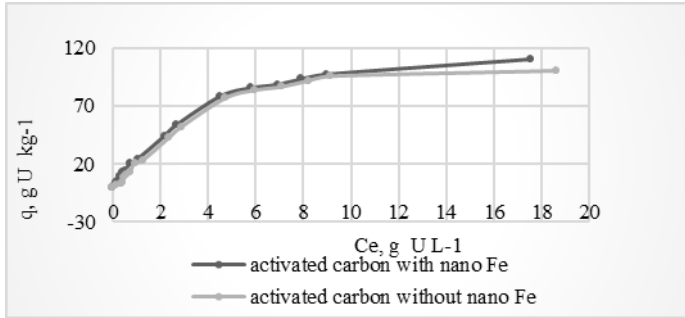


Figure 3. Isotherms for the uranium adsorption on activated carbon Purolite type AC 20 G without/with nano-Fe° impregnated

The Figure 4 and Figure 5 show the Freundlich isotherms for uranium adsorption on activated carbon Purolite AC 20 G without respectively with nano-Fe° impregnated. The slope (1/n) and K_f intercepts of the two isotherms ($\log q_e$ versus $\log C_e$) are determined. After determining the constants K_f and n , Freundlich equations for the two cases are given in Equation (3) and Equation (4):
Activated carbon non-impregnated with nano-Fe°

$$\log q_e = 1.2747 + 1,01048 \log C_e \quad (3)$$

Activated carbon impregnated with nano-Fe°

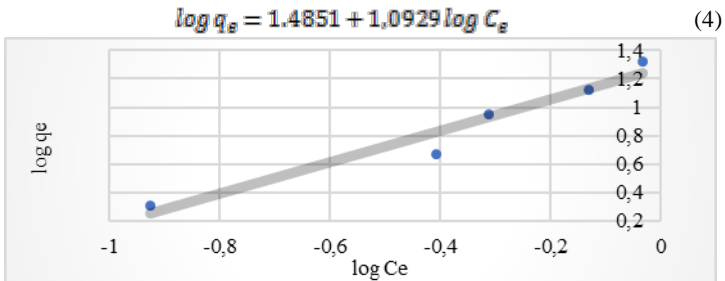


Figure 4. Freundlich isotherm for the adsorption of uranium on activated carbon Purolite AC 20 G non-impregnated with nano-Fe°

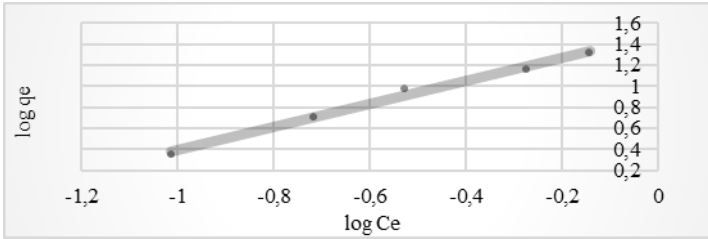


Figure 5. Freundlich isotherm for the adsorption of uranium on activated carbon Purolite AC 20 G impregnated with nano-Fe⁰

R^2 correlation coefficients of 0.9439 and respectively 0.9893 and constant values show that both isothermal experimental data fit well.

The Gibb's free energy (ΔG°) is calculated to evaluate the thermodynamic feasibility of the process (Bhattacharya 2006). The standard free energy can be calculated using Equation (5):

$$\Delta G^\circ = -R \cdot T \cdot \ln K_d \quad (5)$$

Where R ($\text{J mol}^{-1} \text{K}^{-1}$) is the universal gas constant, T (K) is the absolute solution temperature and K_d is the distribution coefficient, calculated by Equation (6):

$$K_d = \frac{q_e}{c_e} \quad (6)$$

The negative value of ΔG° ($-7.734 \text{ kJmol}^{-1}$ for non-impregnated activated carbon with nano-Fe⁰, respectively $-8.294 \text{ KJmol}^{-1}$ for impregnated activated carbon with nano-Fe⁰) establish the feasibility of the sorption process and the spontaneous nature of the adsorption with a high preference of uranium on the activated carbon impregnated with nano-Fe⁰.

Intraparticle diffusion

Experimental data obtained from kinetic studies for the two materials (Figure 6) were processed by applying the Shell Progressive Model for establishing the rate decisive step of the adsorption process.

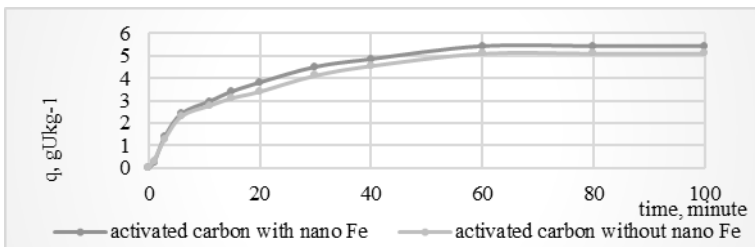


Figure 6. Kinetic curves for the adsorption of uranium on activated carbon Purolite AC 20 G without/with nano-Fe⁰ impregnated

According to the model, the process rate decisive steps are:
External diffusion - Equation (7) :

$$G(X) = \frac{t}{t_0} \quad (7)$$

Internal diffusion - Equation (8) :

$$G(X) = 1 + 3(1 - X)^{2/3} + 2(1 - X) = \frac{t}{t_0} \quad (8)$$

Chemical reaction - Equation (9) :

$$G(X) = 1 - (1 - X)^{1/3} = \frac{t}{t_0} \quad (9)$$

where t (s) is the time, t_0 (s) is the time needed for the reaction to be complete and X (%) is the conversion of activated carbon (progressive achievement of adsorption equilibrium; ratio of adsorption capacity at time, t and maximum adsorption capacity). In Figure 7 and Figure 8 are showed the kinetic equations test results for the three rate decisive steps corresponding of the two types of materials.

In both cases, the chemical reaction and the diffusion through the outer liquid film of the grain are excluded as process rate limiting steps, because their graphic representation is not a straight line for any of the studied coal type.

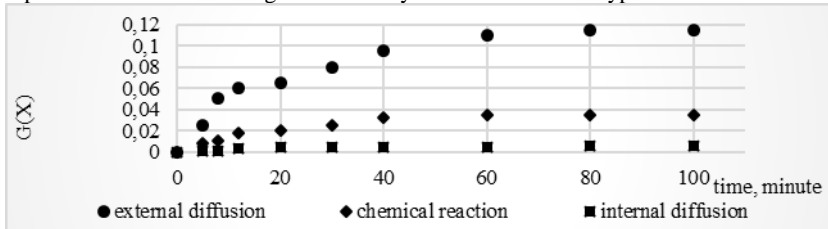


Figure 7. Kinetics of adsorption of uranium and testing of model equations for Shell progressive model for activated carbon Purolite AC 20 G non-impregnated with nano-Fe°

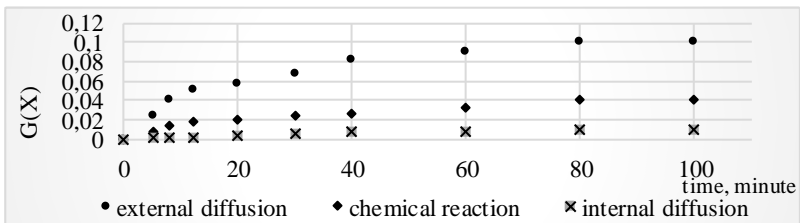


Figure 8. Kinetics of adsorption of uranium and testing of model equations for Shell progressive model for activated carbon Purolite AC 20 G impregnated with nano-Fe°

Linear regression results for the two cases are presented in Table 2 intersection values, slope and linear correlation were determined by MathCAD program.

Table 2. Linear regression values for the batch experiment

Experiment	Applied function	Intersection	Slope	Criteria value Gauss, Ω
AC 20G	X	3.1×10^{-2}	1.176×10^{-3}	3.716×10^{-4}
	$1 - (1 - X)^{1/3}$	10^{-2}	4.089×10^{-4}	4.294×10^{-5}
	$1 - \frac{3(1 - X)^{2/3}}{2(1 - X)}$	4.157×10^{-4}	4.981×10^{-5}	1.799×10^{-7}
AC 20G with nano-Fe ^o	X	2.612×10^{-2}	1.08079×10^{-3}	2.72023×10^{-4}
	$1 - (1 - X)^{1/3}$	8.805×10^{-3}	3.74092×10^{-4}	3.11364×10^{-5}
	$1 - \frac{3(1 - X)^{2/3}}{2(1 - X)}$	2.797×10^{-4}	4.10146×10^{-5}	7.28861×10^{-8}

Linear regression results for internal diffusion, as the rate limiting step of the process, shows a high correlation. Ω functions, adequate of each rate decisive equations represent the standard deviation of experimental values toward the calculated values. The equation for the minimum of the Ω function is the equation which fit best with experimental data, so is the equation which describing kinetic of process. Notice that for the external diffusion and chemical reaction, the deviations are much higher (of order 10^{-4} and 10^{-5}) towards the deviations for the internal diffusion which are of order 10^{-7} or 10^{-8} . The slope values were used to calculate diffusion coefficients using the equation for controlling intraparticle diffusion process. The calculating values of diffusion coefficients are presented in Table 3. These values have size grades in accordance with data presented by other authors referring to cations retention on different supports (Allen & Mckay 1989, Weber & Morris 1963).

Table 3. The calculated values of diffusion coefficients

Type activated carbon	Diffusion coefficient, $m^2 s^{-1}$
Activated carbon Purolite AC 20 G non-impregnated	1.61×10^{-12}
Activated carbon Purolite AC 20 G impregnated with nano-Fe ^o	1.75×10^{-12}

Conclusions

This paper described the equilibrium and the kinetic of uranium adsorption from waste water (from the uranium industry), using activated carbon without/with nano-Fe^o impregnated, applying batch method. For the interpretation of experimental results was used Freundlich model. Calculated values of Freundlich isotherm constants and correlation coefficients R^2 0.9439 for activated carbon Purolite AC 20 G non- impregnated and respectively 0.9893 for activated carbon Purolite AC 20 G

impregnated with nano-Fe⁰ prove the favourable adsorption of uranium on the two solid supports. The negative standard Gibbs energy calculated using distribution coefficient of uranium and spontaneous adsorption establish that the impregnation of iron increase the selectivity of activated carbon for uranium and therefore its retention capacity. Kinetic study (applying the Shell progressive model) showed that intraparticle diffusion is the rate decisive step for uranium adsorption process. The diffusion coefficient value for activated carbon Purolite AC 20 G impregnated with nano-Fe⁰ is greater than for activated carbon non-impregnate, so in the first case, mass transfer resistance is lower and the adsorption process arise easier.

References

- Akperov, E & Maharramov, A 2010, 'Synthesis and uranyl ion adsorption study of cross-linked allyl propionate-maleic anhydride-styrene terpolymer', *Turkish Journal of Chemistry*, vol. 34, pp.99–108.
- Alic, C & Manea, LM 2013, 'Environmental impact due touse of coal in Mintia thermal power plant', *Revista Minelor*, vol. 19, no.1, pp. 2-8.
- Allen, SJ & Mckay, G 1989, 'Intraparticle diffusion of basic dye during adsorption onto Sphagnum Peat', *Journal of Environmental Pollution*, vol. 50, pp.39-50.
- Alvarado, JS & Rose, C 2010, 'Degradation of carbon tetrachloride in the presence of zero-valent iron', *Journal of Environmental Monitoring*, vol. 12, pp.1524-1528.
- Bhattacharya, AK 2006, 'Adsorption of Zn (II) from aqueous solution by using different adsorbents', *Chemical Engineering Journal*, vol. 123, pp. 43-51.
- Bratkova, S & Angelov, A 2013, 'Biotechnogical removal of heavy metals from mining wastewaters by dissimilative sulphate reduction', *Revista Minelor*, vol. 19, no. 3, pp. 22-28.
- Dickinson, M & Scott, TB 2010, 'The application of zero-valent iron nanoparticles for the remediation of a uranium-contaminated waste effluent', *Journal of Hazardous Materials*, vol. 178, pp.171-179.
- Eglal, MM & Ramamurthy, AS 2015, 'Competitive Adsorption and Oxidation Behavior of Heavy Metals on nZVI Coated with TEOS', *Water Environment Research*, vol. 87, no.11, pp. 2018-2026.
- Erust, C & Sahin, M 2014, 'Metal Recovery from Waste by Biological Processes in Urban Mining', *Recycling Industry*, vol.78, no.3, pp. 74-78.
- Gheju, M 2011, 'Hexavalent Chromium Reduction with Zero-Valent Iron (ZVI) in Aquatic Systems', *Water Air Soil Pollution*, vol. 222, pp. 103-107.
- Hu, X & Wang, J 2011, 'Adsorption of chromium (VI) by ethylenediamine-modified cross-linked magnetic chitosan resin: Isotherms, kinetics and thermodynamics', *Journal of Hazardous Materials*, vol. 185, pp. 306-314.
- Khan, AS 2012, 'Theory of adsorption equilibria analysis based on general equilibrium constant expression', *Turkish Journal of Chemistry*, vol. 36, pp. 219-231.
- MacFarlane, JW & Payton, OD 2014, 'Lightweight aerial vehicles for monitoring, assessment and mapping of radiation anomalies', *Journal of Environmental Radioactivity*, vol. 136, no.1, pp. 127–130.
- Mamadou, D & Duncan, JS 2013, 'Nanotechnology Applications for Clean Water', *Journal of Nuclear Materials*, vol. 443, no.1-3, pp. 250-255.

- Mas Haris, MR & Abdul Wahab, NA 2011, 'The sorption of cadmium (II) ions on mercerized rice husk and activated carbon', *Turkish Journal of Chemistry*, vol. 35, pp. 936-950.
- Oprčkal, P & Mladenović, A 2017, 'Critical evaluation of the use of different nanoscale zero-valent iron particles for the treatment of effluent water from a small biological wastewater treatment plant', *Chemical Engineering Journal*, vol. 321, pp. 20-30.
- Panturu, RI, Jinescu, G, Panturu, E, Filcenco-Olteanu, A 2010, 'Synthesis zerovalent iron used for the radioactive contaminated water treatment', *U.P.B Scientific Bulletin, Series B*, vol. 72, pp. 207-219.
- Panturu, RI, Jinescu, G, Panturu, E, Filcenco-Olteanu, A & Radu, AD 2011, 'Arsen-X^{III} Purolite resin used for the depollution of uranium contaminated waters', *Revista de Chimie*, vol. 62, no. 8, pp. 814-817.
- Wang, CB & Zhang, WX 1997, 'Synthesizing Nanoscale Iron Particles for Rapid and Complete Dechlorination of TCE and PCBs', *Environmental Science & Technology*, vol. 31, pp. 2154-2158.
- Weber, W & Morris, J 1963, 'Kinetics of Adsorption on Carbon from solutions', *Journal of the Sanitary Engineering Division*, vol. 89, pp. 31-60.
- Zhang, X 2003, 'Nanoscale iron particles for environmental remediation', *Journal of Nanoparticle Research*, vol.5, pp. 323-327.